Chemistry–A European Journal

Research Article
doi.org/10.1002/chem.202400173

Chemistry Europe
European Chemical Societies Publishing

www.chemeurj.org

Optimal Oriented External Electric Fields to Trigger a Barrierless Oxaphosphetane Ring Opening Step of the Wittig Reaction

Josep Maria Bofill,*[a, b] Marco Severi,*[c] Wolfgang Quapp,*[d] Jordi Ribas-Ariño,*[b, e] Ibério de P. R. Moreira,*[b, e] and Guillermo Albareda*[f]

Dedicated to professor Dr. Miquel Solà Puig in his 60 birthday.

The Wittig reaction is one of the most important processes in organic chemistry for the asymmetric synthesis of olefinic compounds. In view of the increasingly acknowledged potentiality of the electric fields in promoting reactions, here we will consider the effect of the oriented external electric field (OEEF) on the second step of Wittig reaction (i.e. the ring opening oxaphosphetane) in a model system for non-stabilized ylides. In particular, we have determined the optimal direction and strength of the electric field that should be applied to annihilate the reaction barrier of the ring opening through the polarizable molecular electric dipole (PMED) model that we have recently developed. We conclude that the application of the optimal external electric field for the oxaphosphetane ring opening favours a Bestmann-like mechanism.

Introduction

The Wittig reaction is undoubtedly one of the most widely used methods in the synthesis of alkenes.[1] It is also very important in the pharmaceutical industry, where it has been employed as a tool in the asymmetric synthesis of natural products (e.g. vitamin A) and different types of drugs.[2–4] The Wittig reaction occurs between a carbonyl compound (aldehyde or ketone in general) and a phosphonium ylide to furnish a phosphine oxide and an alkene with a high level of stereocontrol.[5] The presence of salts (especially, lithium salts) and the nature of the solvent, among other experimental variables, are known to play an important role in the selectivity of the reaction. Many efforts, using both experimental[6–12] and computational approaches,[12–29] have been devoted to elucidating the mechanism of the Wittig reaction. The currently accepted mechanism entails a formal [2 + 2] cycloaddition that leads to an oxaphosphetane (OP), followed by pseudorotation at phosphorus, and, finally, a ring-opening of the cyclic intermediate, resulting in the generation of the olefin and phosphine oxide. A general description of the Wittig reaction is shown in Figure 1.

In general, the formation of the OP is almost irreversible, and as such, it commonly governs the E/Z selectivity of the olefin.[5] Experimental evidence regarding the involvement of OP in the Wittig process is primarily derived from NMR spectroscopy at low temperatures[30–33] in cases where the ylides are non- or semi-stabilized (R_3PCHR' where R′ = alkyl for non-stabilized and R′ = aryl for semi-stabilized). In a few cases, OPs have even been isolated and structurally characterized by means of X-ray diffraction techniques.[34] In the case of stabilized ylides (R′ = CO_2R''), the corresponding OPs have not yet been observed[11] due to the fast rate at which they furnish the alkene and phosphine oxide. Regarding betaine intermediates, many experimental works have shown that these species are never formed under salt-free conditions.[5,11,35]

The demonstration that oriented external electric fields (OEEFs) can enhance the rate of a Diels-Alder reaction in a landmark scanning tunneling microscopy break-junction (STM-BJ) experiment at the single-molecule level[36] sparked a

[a] Prof. Dr. J. M. Bofill
Departament de Química Inorgànica i Orgànica, Secció de Química Orgànica, Universitat de Barcelona, C/Martí i Franquès 1, 08028 Barcelona, Spain
E-mail: jmbofill@ub.edu

[b] Prof. Dr. J. M. Bofill, Prof. Dr. J. Ribas-Ariño, Prof. Dr. I. d. P. R. Moreira
Institut de Química Teòrica i Computacional (IQTCUB), Universitat de Barcelona, C/Martí i Franquès 1, 08028 Barcelona, Spain
E-mail: j.ribas@ub.edu
i.moreira@ub.edu

[c] M. Severi
Department of Chemistry G. Ciamician, University of Bologna, Via F. Selmi 2, 40126 Bologna, Italy
E-mail: marco.severi6@unibo.it

[d] Dr. W. Quapp
Mathematisches Institut, Universität Leipzig, PF 100920, D-04009 Leipzig, Germany
E-mail: quapp@math.uni-leipzig.de

[e] Prof. Dr. J. Ribas-Ariño, Prof. Dr. I. d. P. R. Moreira
Departament de Ciència de Materials i Química Física, Secció de Química Física, Universitat de Barcelona, C/Martí i Franquès 1, 08028 Barcelona, Spain

[f] Dr. G. Albareda
Ideaded, C/de la Tecnologia 35, 08840 Viladecans, Barcelona, Spain
E-mail: guillealpi@gmail.com

Supporting information for this article is available on the WWW under https://doi.org/10.1002/chem.202400173

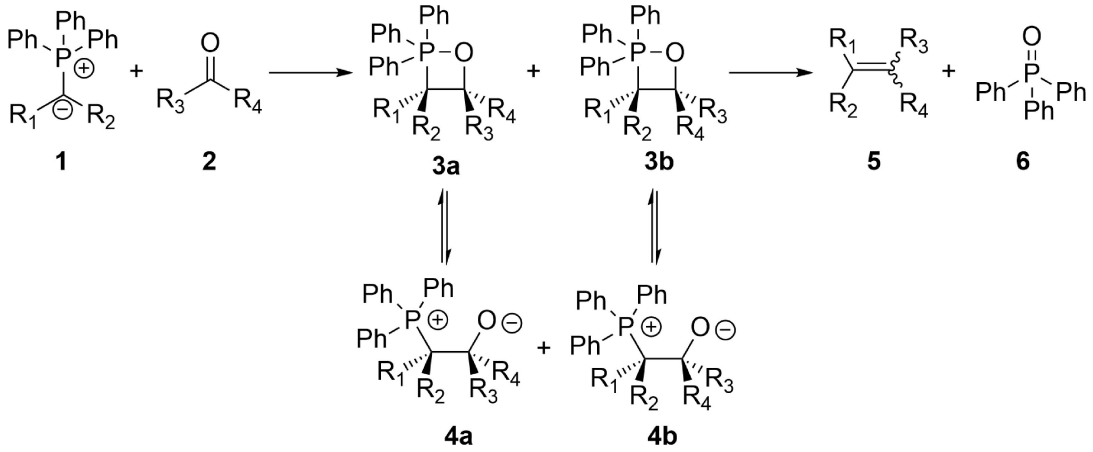

Figure 1. The Wittig reaction. A phosphonium ylide (**1**) and a carbonyl compound (**2**) react either as [2 + 2] cycloaddition or as a nucleophilic attack to form a stable oxaphosphetane (OP) intermediate (**3 a** and **3 b**) that can exhibit an interconversion equilibrium with the corresponding betaine forms (**4 a** and **4 b**). In a subsequent step, the OP evolves to the final phosphine oxide (**5**) and an alkene (**6**) by ring opening, which is usually the limiting step of the mechanism. The Z/E stereochemistry of the alkene product of the Wittig reaction is strongly dependent on the stereochemistry of the reactants and the reaction conditions but usually proceeds with very high stereoselectivity.

renewed interest in the use of oriented external electric fields (OEEFs) as a tool to promote and control chemical reactivity.[37–40] Indeed, subsequent STM-BJ experiments have shown that OEEFs can accelerate other reactions,[41–47] and alternative experimental techniques with greater potential for scalability in utilizing OEEFs have been reported.[48–54] Concurrently with experimental endeavours, significant attention has been devoted to predicting and understanding the effects of OEEFs in reactivity by means of computational studies.[55–76] Remarkably, some of the pioneering computational works were reported much prior to the first experimental evidence of the impact of OEEFs in reactivity.[77–81] Here, we present a computational study aimed at exploring the most efficient way of promoting a Wittig reaction through the utilization of OEEFs. Specifically, we will determine the optimal orientation or direction in which an OEEF should be applied to remove the reaction barrier of the ring-opening step of the Wittig reaction with the smallest possible field strength.

The investigation of the most efficient way of harnessing OEEFs to promote the Wittig reaction will be carried out using the simplest model reaction, namely: $CH_2O + CH_2PMe_3 \rightarrow C_2H_4 + Me_3PO$. This model reaction is shown in Figure 2. As the ylide of this simplified reaction (compound **7** in Figure 2) is of the non-stabilized type, the OP (compound **9**) ring-opening is expected to be the rate-determining step of the overall Wittig reaction. As such, we will exclusively focus on this step of the process.

Despite the relevance of the stereoselectivity in the Wittig reaction, the simplicity of the ylide of our model system precludes any investigation of the effects of an OEEF on the stereoselectivity of the reaction, which is left for further studies. The study of the formation of the betaine intermediate from the heterolytic cleavage of the P–O bond is also out of the scope of the present article because this zwitterionic species has been shown to lie quite above in energy with respect to OP in THF.[82] The investigation of the impact of the OEEF on the relative energy of the betaine is also left for future studies.

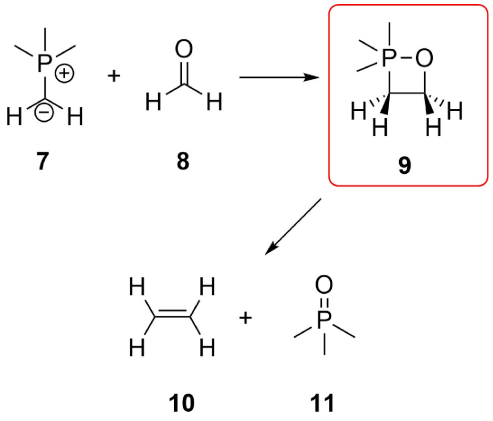

Figure 2. The simplified model of the Wittig reaction studied in this work. The structure of the OP intermediate (compound **9**) is crucial to control the stereochemistry of the resulting alkene and the ring opening is the limiting step of the Wittig reaction. Notice that in this model the absence of stereocenters in the reactants results in an OP structure with C_s symmetry leading to an alkene without Z/E stereochemistry.

The optimal orientation in which an OEEF should be applied to trigger a barrierless OP ring opening will be determined using the so-called polarizable molecular electric dipole (PMED) model, which we have recently reported.[83] In this model, which is based on Optimal Control and Catastrophe theories, the optimal OEEF (oOEEF) is defined as the electric field over a possible set of fields with the smallest possible strength to render a given chemical transformation (i.e. in a given reaction valley of the potential energy surface (PES)) into a barrierless process. Accordingly, the PMED model provides the optimal field in strength and direction to annihilate a given chemical barrier by considering the contributions of both the inherent dipole and field-induced dipole (arising from the electric polarizability) of the molecular system.

This article is structured as follows. In the Methodology section, we will summarize the main features of the PMED model and will provide details of the electronic structure

calculations that have been carried out for the model Wittig reaction described in Figure 2. In the Results Section, we will first discuss the most important aspects of the ring-opening of the OP at zero field and we will then focus on the determination of the oOEEF for this reaction, paying special attention to the role of symmetry.

Methodology

The PMED model considers that the effect of an OEEF on a given reaction can be described by the following perturbed PES:

$$\begin{aligned} V_{\mathbf{e}_n}(\mathbf{x}, E) &= V(\mathbf{x}) + P_{\mathbf{e}_n}(\mathbf{x}, E) \\ &= V(\mathbf{x}) - E\mathbf{e}_n^T\{\mathbf{d}(\mathbf{x}) + 1/2\,\mathbf{A}(\mathbf{x})E\mathbf{e}_n\} \end{aligned} \tag{1}$$

where $V(\mathbf{x})$ is the original or unperturbed PES of molecular system, $\mathbf{d}(\mathbf{x})$ and $\mathbf{A}(\mathbf{x})$ are the inherent dipole and polarizability of the molecular system, respectively, E is the strength of the electric field acting on the system and $\mathbf{e}_n$ is the direction of the field.

The *optimal bond breaking point* or *optimal barrier breakdown point* (oBBP) is one of the key concepts of the PMED model. The oBBP of a given reaction is a special point of the PES that lies somewhere in between the reactant configuration and the transition state (TS) configuration. As shown in Refs. [84] and [85], this point satisfies the following condition:

$$\mathbf{H}(\mathbf{x})\mathbf{g}(\mathbf{x})\big|_{\mathbf{x}=\mathbf{x}_{oBBP}} = \mathbf{0} \quad \mathbf{g}(\mathbf{x})\big|_{\mathbf{x}=\mathbf{x}_{oBBP}} \neq \mathbf{0} \tag{2}$$

where $\mathbf{H}(\mathbf{x}_{oBBP})$ is the Hessian of the original PES at the oBBP and $\mathbf{g}(\mathbf{x}_{oBBP})$ is the gradient of the original PES at the oBBP. The point along the intrinsic reaction coordinate (IRC) curve joining the reactant and TS configurations is commonly a good starting point for the location of the oBBP using the algorithms presented in Refs. [85] and [86]. After the location of the oBBP, the oOEEF can be determined by imposing the two following conditions: i) the Hessian matrix of the perturbed PES must be equal to the Hessian matrix of the original PES at the oBBP; ii) the gradient is an eigenvector of the Hessian matrix of the perturbed PES. After determination of the oOEEF at the oBBP, the force displacement stationary point (FDSP) path is computed from the oBBP forward and backward in the direction of $\mathbf{g}(\mathbf{x}_{oBBP})$, since the unperturbed gradient at the oBBP coincides with the tangent of the FDSP curve at this point. The FDSP path is obtained by integration of the following equation:[83,87,88]

$$\mathbf{H}_{\mathbf{e}_n}(\mathbf{x}, E)\left(\frac{d\mathbf{x}}{dt}\right) = \mathbf{r}_{\mathbf{e}_n}(\mathbf{x}, E)\left(\frac{dE}{dt}\right) \tag{3}$$

where, $d\mathbf{x}/dt$, is the tangent of the path, dE/dt, accounts the change of the field strength through the path and $\mathbf{r}_{\mathbf{e}_n}(\mathbf{x}, E)$ is the derivative of the perturbed PES with respect to $\mathbf{x}$ and the field strength E. We recall that at the oBBP, $dE/dt = 0$, and, $(d\mathbf{x}, dt)\big|_{\mathbf{x}=\mathbf{x}_{oBBP}} = \mathbf{g}(\mathbf{x}_{oBBP})$. It is worth noting that Eq. (3) is a generalization of the Newton trajectory equation used as a model in mechanochemistry. The reader is referred to Table 1 of Ref. [87] for further details and comparisons.

The gas-phase PES of the model Wittig reaction between $CH_2O + CH_2PMe_3$, together with the electric dipole moments and polarizabilities, were calculated using the B3LYP functional[89–92] and the 6-31G* basis set,[93] as implemented in the ORCA code (version 5.0.3).[94–99] Grimme's D3BJ dispersion correction[100,101] was employed in all calculations. The oBBP and oOEEF were obtained using MANULS code,[102] an open-source Python code where the PMED algorithm described in Ref. [83] is implemented. The MANULS code is available in https://github.com/MSeveri96/MANULS. The first and second derivatives of the energy, dipole, and polarizability with respect to the subset of internal coordinates chosen to explore the reaction (see below) were calculated numerically in the MANULS code with a central differences approach.

Results

We will first set the stage by analyzing the main features of the Wittig reaction between $CH_2O + CH_2PMe_3$ at zero field. The relevant structures corresponding to the stationary points of the PES are shown in Figure 3. As mentioned in the Introduction, we will focus exclusively on the ring-opening of OP because this is the rate-determining step of the Wittig process when dealing with non-stabilized ylides. In the computational study of Harvey and coworkers (Ref. [20]), the barrier for the OP formation is reported to be lower than 1 kcal mol^{-1} (at the B3LYP/6-31G* level), which means that this reaction readily takes place without any need of promoting it. In the most stable conformation of the OP intermediate (see OP conformation 1 in Figure 3a), the coordination geometry around phosphorous is a trigonal bipyramid, and the oxygen coming from the aldehyde is in the apical position. Yet, as shown in Ref. [20], this is not the conformation that undergoes ring

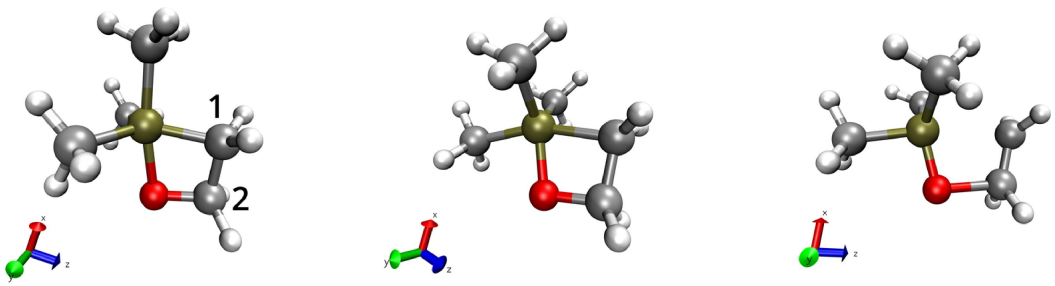

(a) *OP conformation 1* **(b)** *OP conformation 2* **(c)** *Transition state*

Figure 3. Panels a–b) correspond to a stereochemical formula of the two minimal conformations on the PES of oxaphosphetane (OP), panel c) corresponds to a stereochemical formula of the transition state. Panel a) also shows the numbering of the carbon atoms used in this work.

opening. The conformation that leads to the final product via ring opening has an ylidic carbon in the apical position. In this conformation (see OP conformation 2 in Figure 3b), which lies less than 2.0 kcal mol^{-1} above than conformation 1, the four atoms of the ring lie in the same plane. In fact, the optimized structure of conformation 2 is very close to being a C_s geometry.

The transition state (TS) structure (see Figure 3c) that connects the conformation 2 of OP with the final products possesses a C_s symmetry too. This TS structure lies 19.1 kcal mol^{-1} above the reactants. As previously shown in Ref. [20], the reaction proceeds via an asynchronous TS, in which the P–C bond is almost broken but the C–O bond is still quite short. Given that both the reactant and TS configurations have C_s symmetry, the oBBP configuration of the reaction is expected to display C_s symmetry too.

As explained in the previous section, the determination of the oOEEF for a given reaction requires the location of the corresponding oBBP. The location of the oBBP and the subsequent determination of the oOEEF are expensive calculations when working in the full dimensional space. For this reason, we have opted for working on the two-dimensional subspace defined by P–C_1 and C_2–O (see Figure 3a for C labels) bond distances, which are the two internal coordinates that undergo a largest change upon ring opening of OP. The original PES of the reaction in this subspace is displayed in Figure 4. This plot was obtained by scanning the P–C_1 bond from 1.9 to 3.5 Å and the C_2–O bond from 1.4 to 2.7 Å with a step of 0.1 Å.

The minimum reactant structure associated with conformation 2 of OP (see Figure 4) is located at the bottom-left region of the 2D plot. The TS is located along the diagonal of the 2D plot, at longer P–C_1 and C_2–O bond distances. The curve depicted by black points marks the intrinsic reaction coordinate (IRC) path joining the OP reactant and the Wittig products.

The location of the oBBP was carried out using a finer mesh of the 2D PES in the region of interest. Specifically, the region that was scanned spans values from 1.95 to 2.5 Å for the P–C_1 bond and values from 1.45 to 1.80 Å for the C_2–O bond with a step of 0.025 Å. The initial configuration for the location of the oBBP in this finer mesh was the IRC point with the highest value of gradient norm. The oBBP configuration is marked with a red point in the Figures 4a and 4b. The molecular structure of the oBBP, as shown in Figure 5, is much closer to the reactant, OP, than the TS. In fact, the C_2–O distance at the oBBP (1.475 Å) remains almost unchanged with respect to OP, whereas the P–C_1 bond is significantly larger (2.275 Å). Remarkably, the structure of the oBBP hints at a Bestmann-type mechanism.[103] We recall that in the Bestmann mechanism, the P–C_1 bond breaks in the first stage of the ring opening of the OP, thereby leading to a zwitterionic-like structure in which the C_2–O bond remains almost unchanged. This structure then transforms into the final products of the Wittig reaction through the cleavage of the C_2–O bond.

As explained in the Methodology section, the oBBP configuration permits the derivation of the oOEEF. According to our calculations, the normalized direction of the oOEEF for the OP ring opening lies in the plane containing the P–O–C_2–C_1

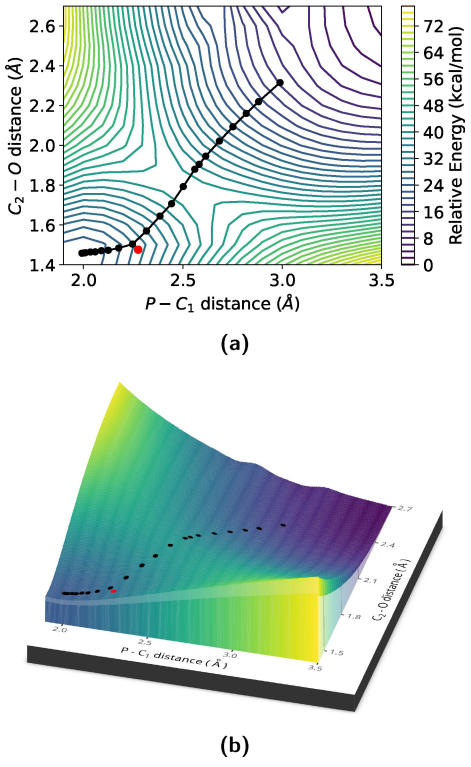

Figure 4. Two- (a) and three-dimensional (b) plots of the original or unperturbed PES in the subspace characterized by the C–P and C–O bond distances. The bond distances are given in Å. The set of black dots are points of the IRC curve. The red dot indicates the position of the optimal BBP (oBBP). The energy is relative to the minimum of the PES. The energy is given in kcal/mol. (Note: could you please enlarge the image corresponding to figure 4b, so that the axes are clearly readable?).

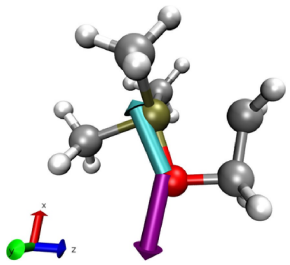

Figure 5. Representation of the molecular geometry in the oBBP. The purple arrow shows the direction of the oOEEF, which is given by the vector, $\mathbf{e}_n = (-0.958, -0.222, -0.184)$, in the reference system defined by the Cartesian axes plotted in the Figure and used in the Supplementary Information. The cyan arrow shows the direction of the molecular dipole moment vector.

atoms and forms angles of 49° and 115° with the O–P and C_2–O bonds, respectively. The amplitude of the oOEEF is in turn, $E = 0.0798$ a.u. $= 4.10$ V/Å. The orientation of the optimal field as well as the orientation of the inherent dipole at the oBBP are depicted in Figure 5. It is worth noting that if we had done the calculations without taking into account the polarizability tensor (i.e., ignoring the term with $\mathbf{A}(\mathbf{x})$ in Eq. (1), the normalized direction of the oOEEF would form the same angle with the O–P and C_2–O bonds, but the amplitude would increase up to 4.80 V/Å. It thus follows that polarizability does

not change the direction of the oOEEF, but results in a significant decrease of the field strength required to make the ring opening barrierless. It is also worth mentioning that a numerical test performed at the geometry of the oBBP along the optimal oOEEF shows that the contribution of the first higher hyperpolarizability term is negligible (< 1 %, see Supporting Information for details) at the field = 4.10 V/Å. Therefore, the expansion until second order with respect to E of $P_{e_n}(\mathbf{x}, E)$ function given in Eq. (1) is valid for this specific system.

The perturbed PES, see Eq. (1), resulting from the application of the oOEEF to the unperturbed system is displayed in Figure 6. This perturbed PES confirms that the oOEEF flattens the region around the oBBP especially along the P–C_1 bond until this bond is completely broken. At this point the cleavage of the C_2–O bond starts and the system evolves toward the Wittig region products. This evolution under the influence of the external electric field is reminiscent of the Bestmann mechanism.[103] Therefore, our results not only show that an electric field can promote the ring opening of oxophosphetanes, but also that the field can change the underlying reaction mechanism.

Admittedly, a field strength of 4.10 V/Å is larger than those usually applied in currently available setups of STM. However, this strength is not that large compared with the standard fields applied in STM experiments. Indeed, field strengths of 2 V/Å have been reported[104] and fields of the order of 5 V/Å, although extreme, are suitable for standard STM experimental setups.[48,105,106] Furthermore, let us stress that even if the strength of the oOEEF cannot be achieved in experiment, the activation energy will decrease in the most efficient way following the direction of the oOEEF. In fact, the barrier with a field of 2 V/Å with the oOEEF direction can be estimated by using Eq. (1) computed in the two-dimensional PES model in Figure 4. Using this procedure, it is found that the barrier of the reaction at 2 V/Å is 11.1 kcal mol^{-1}, which is substantially smaller than the barrier at zero field (19.1 kcal mol^{-1}). Remarkably, the perturbed PES with a field strength of 2 V/Å is still consistent with a Bestmann-like mechanism (see Supporting Information).

It should also be mentioned that even if a field strength of 4.10 V/Å is achieved in a STM experiment, such a strong field could compromise the stability of the final products (e.g. larger fields could even trigger different ionization processes). In fact, a geometry optimization performed in the full-dimensional space (i.e. taking into account all the structural degrees of freedom) using the oBBP as starting configuration and with the explicit inclusion of the oOEEF shows that the ring-opening takes place but that the P–C bonds of the phosphine oxide break later on. Remarkably, the ethylene molecule, which is the most relevant product of the Wittig reaction, is stable in these conditions.

Finally, the large field strength required to annihilate the barrier might have an impact on other steps of the reaction. Particularly relevant is the impact of the electric field on the equilibrium between OP and the betaine specie. Indeed, a large stabilization of the betaine with respect to the OP would be detrimental to the formation of ethylene. According to our calculations,[1] the energy of the betaine lies *ca.* 12 kcal mol^{-1} above the energy of the OP reactant in the presence of the oOEEF. This can be understood by comparing the inherent dipole moment vector of the oBBP with that of the betaine-like geometry. Indeed, the large angle formed by these two dipoles (~45°) indicates that the electronic structures of these two molecular geometries are very different. Therefore, the field-induced stabilization of the oBBP does not result in a stabilization of the betaine-like molecular geometry. The fact that a hypothetical involvement of a betaine pathway can be disregarded further supports the conclusion that the field-induced ring-opening of OP proceeds by means of a Bestmann-like mechanism.

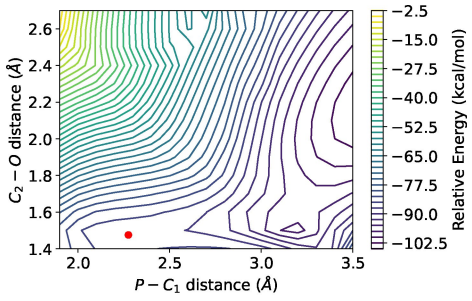

(a)

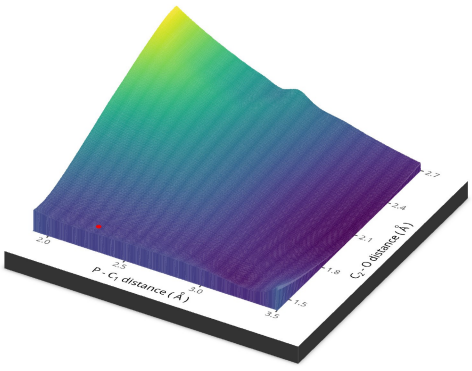

(b)

Figure 6. Two- (a) and three-dimensional (b) plots of perturbed PES. The red dot is the oBBP. The energy is relative to the minimum of the unperturbed PES. Note: could you please enlarge the image corresponding to figure 6b, so that the axes are clearly readable?).

Conclusions

We have determined the optimal direction in which an external electric field should be applied to enhance the ring opening of oxaphosphetane in a model system of the Wittig reaction for non-stabilized ylides by means of PMED model that we have recently developed.[83] An optimal electric field lying on the plane containing the 4 atoms of the oxaphosphetane ring and

[1] Note that in gas phase and in the absence of any OEEF, the specific betaine associated with the Wittig reaction herein studied does not have a minimum energy configuration in the potential energy surface. Still, we have assessed the impact of the oOEEF on a betaine-like configuration that has been generated by elongating the P–O bond of the reactants geometry, resulting in a P–O distance of 2.2 Å.

forming an angle around 45° with respect to the O–P bond, with a strength slightly larger than 4 V/Å, renders the ring opening an almost barrierless process.

A comparison between the non-perturbed and perturbed energy surfaces for the ring opening of the oxaphosphetane reveals that the external electric field has an important impact in the reaction mechanism. At zero field, i. e. non-perturbed PES, the reaction proceeds through a one-step non synchronous process, where the P–C bond is more elongated than the O–C bond. In the presence of the optimal electric field, instead, the degree of non-synchronicity is much higher because the P–C bond breaks prior to cleavage of O–C bond. Accordingly, the optimal electric field favours a Bestmann-like mechanism[103] for the oxaphosphetane ring opening.

Acknowledgements

The authors thank the financial support from the Spanish Ministerio de Economía y Competitividad, Project Nos. PID2019-109518GB-I00, PID2020-117803GB-I00; Spanish Structures of Excellence María de Maeztu program, through Grant No. CEX2021-001202-M. Agència de Gestió d'Ajuts Universitaris i de Recerca de Generalitat de Catalunya, Project No. Projecte 2021 SGR 00354. We acknowledge the CINECA award under the ISCRA initiative, for the availability of high-performance computing resources and support.

Conflict of Interests

The authors declare no conflict of interest.

Data Availability Statement

The data that support the findings of this study are available in the supplementary information of this article.

Keywords: optimal oriented external electric field · catastrophe theory in chemistry · control theory in chemistry · barrier breakdown · force displaced stationary points · wittig reaction

[1] G. Wittig, G. Geissler, *Justus Liebigs Ann. Chem.* **1953**, *580*, 44.
[2] H. Pommer, *Angew. Chem. Int. Ed. Engl.* **1977**, *16*, 423.
[3] K. C. Nicolaou, M. W. Härter, J. L. Gunzner, A. Nadin, *Liebigs Ann.* **1997**, *1997*, 1283.
[4] M. M. Heravi, V. Zadsirjan, M. Daraie, M. Ghanbarian, *ChemistrySelect* **2020**, *5*, 9654.
[5] E. Vedejs, M. J. Peterson, Stereochemistry and Mechanism in the Wittig Reaction, pages 1–157, John Wiley & Sons, Ltd **1994**.
[6] E. Vedejs, C. F. Marth, *J. Am. Chem. Soc.* **1988**, *110*, 3948.
[7] E. Vedejs, T. J. Fleck, *J. Am. Chem. Soc.* **1989**, *111*, 5861.
[8] E. Vedejs, C. F. Marth, *J. Am. Chem. Soc.* **1989**, *111*, 1519.
[9] B. E. Maryanoff, A. B. Reitz, *Chem. Rev.* **1989**, *89*, 863.
[10] P. A. Byrne, D. G. Gilheany, *J. Am. Chem. Soc.* **2012**, *134*, 9225.
[11] P. A. Byrne, D. G. Gilheany, *Chem. Soc. Rev.* **2013**, *42*, 6670.
[12] J. García López, P. M. Sansores Peraza, M. J. Iglesias, L. Roces, S. García-Granda, F. López Ortiz, *J. Org. Chem.* **2020**, *85*, 14570.
[13] F. Mari, P. M. Lahti, W. E. McEwen, *Heteroat. Chem.* **1990**, *1*, 255.
[14] F. Mari, P. M. Lahti, W. E. McEwen, *Heteroat. Chem.* **1991**, *2*, 265.
[15] F. Mari, P. M. Lahti, W. E. McEwen, *J. Am. Chem. Soc.* **1992**, *114*, 813.
[16] H. Yamataka, T. Hanafusa, S. Nagase, T. Kurakake, *Heteroat. Chem.* **1991**, *2*, 465.
[17] A. A. Restrepo-Cossío, H. Cano, F. Marx, C. A. González, *Heteroat. Chem.* **1997**, *8*, 557–569.
[18] H. Yamataka, S. Nagase, *J. Am. Chem. Soc.* **1998**, *120*, 7530.
[19] R. Robiette, J. Richardson, V. K. Aggarwal, J. N. Harvey, *J. Am. Chem. Soc.* **2005**, *127*, 13468.
[20] R. Robiette, J. Richardson, V. K. Aggarwal, J. N. Harvey, *J. Am. Chem. Soc.* **2006**, *128*, 2394.
[21] M. Stępień, *J. Org. Chem.* **2013**, *78*, 9512.
[22] N. Jarwal, J. S. Meena, P. P. Thankachan, *Comput. Theor. Chem.* **2016**, *1093*, 29.
[23] K. Ayub, R. Ludwig, *RSC Adv.* **2016**, *6*, 23448.
[24] Z. Chen, Y. Nieves-Quiñones, J. R. Waas, D. A. Singleton, *J. Am. Chem. Soc.* **2014**, *136*, 13122.
[25] T. Thiemann, *Mini-Rev. Org. Chem.* **2018**, *15*, 412.
[26] P. Farfán, S. Gómez, A. Restrepo, *Chem. Phys. Lett.* **2019**, *728*, 153.
[27] P. Farfán, S. Gómez, A. Restrepo, *J. Org. Chem.* **2019**, *84*, 14644.
[28] E. Chamorro, M. Duque-Noreña, N. Gutiérrez- Sánchez, E. Rincón, L. R. Domingo, *J. Org. Chem.* **2020**, *85*, 6675.
[29] A. Adda, R. H. Aoul, H. Sediki, M. Sehailia, A. M. Krallafa, *Theor. Chem. Acc.* **2023**, *142*.
[30] E. Vedejs, K. A. J. Snoble, *J. Am. Chem. Soc.* **1973**, *95*, 5778.
[31] A. B. Reitz, M. S. Mutter, B. E. Maryanoff, *J. Am. Chem. Soc.* **1984**, *106*, 1873.
[32] B. E. Maryanoff, A. B. Reitz, M. S. Mutter, R. R. Inners, H. R. Almond, *J. Am. Chem. Soc.* **1985**, *107*, 1068.
[33] P. A. Byrne, J. Muldoon, Y. Ortin, H. Müller-Bunz, D. G. Gilheany, *Eur. J. Org. Chem.* **2013**, *2014*, 86.
[34] F. López-Ortiz, J. López, R. Manzaneda, I. Álvarez, *Mini-Rev. Org. Chem.* **2004**, *1*, 65.
[35] M. Appel, S. Blaurock, S. Berger, *Eur. J. Org. Chem.* **2002**, *2002*, 1143.
[36] A. C. Aragonés, N. L. Haworth, N. Darwish, S. Ciampi, N. J. Bloomfield, G. G. Wallace, I. Díez-Pérez, M. L. Coote, *Nature* **2016**, *531*, 88.
[37] S. Shaik, D. Mandal, R. Ramanan, *Nat. Chem.* **2016**, *8*, 1091.
[38] S. Shaik, R. Ramanan, D. Danovich, D. Mandal, *Chem. Soc. Rev.* **2018**, *47*, 5125.
[39] S. Shaik, D. Danovich, J. Joy, Z. Wang, T. Stuyver, *J. Am. Chem. Soc.* **2020**, *142*, 12551.
[40] F. Che, J. T. Gray, S. Ha, N. Kruse, S. L. Scott, J.-S. McEwen, *ACS Catal.* **2018**, *8*, 5153.
[41] L. Zhang, E. Laborda, N. Darwish, B. B. Noble, J. H. Tyrell, S. Pluczyk, A. P. Le Brun, G. G. Wallace, J. González, M. L. Coote, S. Ciampi, *J. Am. Chem. Soc.* **2018**, *140*, 766.
[42] X. Huang, C. Tang, J. Li, L.-C. Chen, J. Zheng, P. Zhang, J. Le, R. Li, X. Li, J. Liu, Y. Yang, J. Shi, Z. Chen, M. Bai, H.-L. Zhang, H. Xia, J. Cheng, Z. Tian, W. Hong, *Sci. Adv.* **2019**, *5*.
[43] Y. Zang, T. Zou, Fu, F. Ng, B. Fowler, J. Yang, H. Li, M. L. Steigerwald, C. Nuckolls, L. Venkataraman, *Nat. Commun.* **2019**, *10*, 4482.
[44] J. Lin, Y. Lv, K. Song, X. Song, H. Zang, P. Du, Y. Zang, D. Zhu, *Nat. Commun.* **2023**, *14*.
[45] B. Zhang, C. Schaack, C. R. Prindle, E. A. Vo, M. Aziz, M. L. Steigerwald, T. C. Berkelbach, C. Nuckolls, L. Venkataraman, *Chem. Sci.* **2023**, *14*, 1769.
[46] X. Wang, B. Zhang, B. Fowler, L. Venkataraman, T. Rovis, *J. Am. Chem. Soc.* **2023**, *145*, 11903.
[47] C. Yang, Z. Liu, Y. Li, S. Zhou, C. Lu, Y. Guo, M. Ramírez, Q. Zhang, Y. Li, Z. Liu, K. N. Houk, D. Zhang, X. Guo, *Sci. Adv.* **2021**, *7*.
[48] S. Ciampi, N. Darwish, H. M. Aitken, I. Díez-Pérez, M. L. Coote, *Chem. Soc. Rev.* **2018**, *47*, 5146.
[49] M. Akamatsu, N. Sakai, S. Matile, *J. Am. Chem. Soc.* **2017**, *139*, 6558.
[50] Y. B. Vogel, L. Zhang, N. Darwish, V. R. Gonçales, A. Le Brun, J. J. Gooding, A. Molina, G. G. Wallace, M. L. Coote, J. González, S. Ciampi, *Nat. Commun.* **2017**, *8*, 2066.
[51] C. F. Gorin, E. S. Beh, Q. M. Bui, G. R. Dick, M. W. Kanan, *J. Am. Chem. Soc.* **2013**, *135*, 11257.
[52] M. Klinska, L. M. Smith, G. Gryn'ova, M. G. Banwell, M. L. Coote, *Chem. Sci.* **2015**, *6*, 5623.
[53] M. T. Blyth, M. L. Coote, *J. Org. Chem.* **2019**, *84*, 1517.
[54] N. G. Léonard, R. Dhaoui, T. Chantarojsiri, J. Y. Yang, *ACS Catal.* **2021**, *11*, 10923.

[55] S. Shaik, T. Stuyver (Editors), *Effects of Electric Fields on Structure and Reactivity*, Theoretical and Computational Chemistry Series, The Royal Society of Chemistry **2021**.
[56] T. Stuyver, D. Danovich, J. Joy, S. Shaik, *WIREs Comput. Mol. Sci.* **2020**, *10*, e1438.
[57] Z. Wang, D. Danovich, R. Ramanan, S. Shaik, *J. Am. Chem. Soc.* **2018**, *140*, 13350.
[58] H. M. Aitken, M. L. Coote, *Phys. Chem. Chem. Phys.* **2018**, *20*, 10671.
[59] K. Bhattacharyya, S. Karmakar, A. Datta, *Phys. Chem. Chem. Phys.* **2017**, *19*, 22482.
[60] S. Yu, P. Vermeeren, T. A. Hamlin, F. M. Bickelhaupt, *Chem. Eur. J.* **2021**, *27*, 5683.
[61] P. Besalú-Sala, M. Solà, J. M. Luis, M. Torrent-Sucarrat, *ACS Catal.* **2021**, *11*, 14467.
[62] R. Ramanan, D. Danovich, D. Mandal, S. Shaik, *J. Am. Chem. Soc.* **2018**, *140*, 4354.
[63] E. J. Mattioli, A. Bottoni, F. Zerbetto, M. Calvaresi, *J. Phys. Chem. C* **2019**, *123*, 26370.
[64] T. Stuyver, D. Danovich, F. De Proft, S. Shaik, *J. Am. Chem. Soc.* **2019**, *141*, 9719.
[65] J. Joy, T. Stuyver, S. Shaik, *J. Am. Chem. Soc.* **2020**, *142*, 3836.
[66] C. Acosta-Silva, J. Bertrán, V. Branchadell, A. Oliva, *ChemPhysChem* **2020**, *21*, 295.
[67] Y. Chen, Y. Liu, Q. Zhang, Y. Yan, W. Yin, *J. Theor. Comput. Chem.* **2020**, *19*, 2050004.
[68] J. Wu, T. Long, H. Wang, J.-X. Liang, C. Zhu, *Front. Chem.* **2022**, *10*, 896944.
[69] F. Che, J. T. Gray, S. Ha, J.-S. McEwen, *ACS Catal.* **2017**, *7*, 551.
[70] E. M. Kempfer-Robertson, L. M. Thompson, *J. Phys. Chem. A* **2020**, *124*, 3520.
[71] K. Jutglar Lozano, R. Santiago, J. Ribas-Ariño, S. T. Bromley, *Phys. Chem. Chem. Phys.* **2021**, *23*, 3844.
[72] T. Stuyver, S. Shaik, *J. Org. Chem.* **2021**, *86*, 9030.
[73] M. Zhang, W. Li, Z. Zhou, S. Zhuo, Z. Su, *ACS Omega* **2022**, *7*, 5782.
[74] H. R. Kelly, P. E. Videla, C. P. Kubiak, T. Lian, V. S. Batista, *J. Phys. Chem. C* **2023**, *127*, 6733.
[75] D. J. Hanaway, C. R. Kennedy, *J. Org. Chem.* **2023**, *88*, 106.
[76] P. Besalú-Sala, A. A. Voityuk, J. M. Luis, M. Solà, *J. Chem. Phys.* **2023**, *158*, 244111.
[77] J. Andrés, A. Lledós, M. Duran, J. Bertrán, *Chem. Phys. Lett.* **1988**, *153*, 82.
[78] E. Carbonell, M. Duran, A. Lledós, J. Bertrán, *J. Phys. Chem.* **1991**, *95*, 179.
[79] R. Meir, H. Chen, W. Lai, S. Shaik, *ChemPhysChem* **2010**, *11*, 301.
[80] S. Shaik, S. P. de Visser, D. Kumar, *J. Am. Chem. Soc.* **2004**, *126*, 11746.
[81] H. Hirao, H. Chen, M. A. Carvajal, Y. Wang, S. Shaik, *J. Am. Chem. Soc.* **2008**, *130*, 3319.
[82] J. García López, P. M. Sansores Peraza, M. J. Iglesias, L. Roces, S. García-Granda, F. López Ortiz, *J. Org. Chem.* **2020**, *85*, 14570.
[83] J. M. Bofill, M. Severi, W. Quapp, J. Ribas-Ariño, I. de P. R. Moreira, G. Albareda, *J. Chem. Phys.* **2023**, *159*, 114112.
[84] W. Quapp, J. M. Bofill, *Theor. Chem. Acc.* **2016**, *135*, 113.
[85] J. M. Bofill, J. Ribas-Ariño, S. P. García, W. Quapp, *J. Chem. Phys.* **2017**, *147*, 152710.
[86] J. M. Bofill, R. Valero, J. Ribas-Ariño, W. Quapp, *J. Chem. Theory Comput.* **2021**, *17*, 996.
[87] J. M. Bofill, W. Quapp, G. Albareda, I. de P. R. Moreira, J. Ribas-Ariño, *J. Chem. Theory Comput.* **2022**, *18*, 935.
[88] J. M. Bofill, W. Quapp, G. Albareda, I. de P. R. Moreira, J. Ribas-Ariño, M. Severi, *Theor. Chem. Acc.* **2023**, *142*, 22.
[89] A. D. Becke, *J. Chem. Phys.* **1993**, *98*, 5648.
[90] C. Lee, W. Yang, R. G. Parr, *Phys. Rev. B* **1988**, *37*, 785.
[91] S. H. Vosko, L. Wilk, M. Nusair, *Can. J. Phys.* **1980**, *58*, 1200.
[92] P. J. Stephens, F. J. Devlin, C. F. Chabalowski, M. J. Frisch, *J. Phys. Chem.* **1994**, *98*, 11623.
[93] W. J. Hehre, R. Ditchfield, J. A. Pople, *J. Chem. Phys.* **1972**, *56*, 2257.
[94] F. Neese, *WIREs Comput. Mol. Sci.* **2012**, *2*, 73.
[95] F. Neese, *WIREs Comput. Mol. Sci.* **2018**, *8*, e1327.
[96] F. Neese, F. Wennmohs, U. Becker, C. Riplinger, *J. Chem. Phys.* **2020**, *152*, 224108.
[97] F. Neese, *WIREs Comput. Mol. Sci.* **2022**, *12*, e1606.
[98] F. Neese, *J. Comput. Chem.* **2023**, *44*, 381.
[99] F. Neese, F. Wennmohs, A. Hansen, U. Becker, *Chem. Phys.* **2009**, *356*, 98.
[100] S. Grimme, J. Antony, S. Ehrlich, H. Krieg, *J. Chem. Phys.* **2010**, *132*, 154104.
[101] S. Grimme, S. Ehrlich, L. Goerigk, *J. Comput. Chem.* **2011**, *32*, 1456.
[102] J. M. Bofill, W. Quapp, J. Ribas-Ariño, M. Severi, G. Albareda, I. de P. R. Moreira, MANULS (Make chemicAl reactioNs spontaneoUs via optimaL fieldS).
[103] H. J. Bestmann, *Pure Appl. Chem.* **1980**, *52*, 771.
[104] J. A. Stroscio, D. M. Eigler, *Science* **1991**, *254*, 1319.
[105] A. C. Aragonés, N. Darwish, S. Ciampi, F. Sanz, J. J. Gooding, I. Díez-Pérez, *Nat. Commun.* **2017**, *8*, 15056.
[106] A. C. Aragonés, private communication. **2024**.

Manuscript received: January 15, 2024
Accepted manuscript online: March 8, 2024
Version of record online: April 9, 2024